**Hassen BELILA[1], Nasserdine BOUDJERDA[2], Ahsene BOUBAKIR[2], Imen BAHRI[3]**

University of Oum El Bouaghi, Algeria (1), University Mohammed Seddik Ben Yahia Jijel, Algeria (2), University of Paris-Saclay, France (3)

doi:10.15199/48.2020.10.29

# Improved STATCOM efficiency using a hybrid technique based on sliding mode control and proportional integral control

***Abstract**. Static compensators of reactive power (STATCOMs) are among the most efficient devices for improving the network power quality. The efficiency of such devices is largely determined by the used automatic control technique. In this work, we propose an advanced hybrid algorithm based on Sliding Mode Control (SMC) combined with classical proportional-Integral (PI) technique. To show the efficiency of the proposed method, a comparison with the traditional PI control is performed. The comparison focused mainly on dynamic performance and grid harmonic pollution.*

*Streszczenie. Jakość działania kompensatora mocy biernej STATCOM zależy od właściwości układu automatycznego sterowania. W pracy zaprezentowano hybrydowy algorytm bazujący na sterowaniu ślizgowym współpracujący z klasycznym sterownikiem PI. **Poprawa skuteczności STATCOM przez zastosowanie algorytmu hybrydowego będącego kombinacją na sterowania ślizgowego i regulatora PI***

**Keywords:** STATCOM, Sliding Mode Control, PI control, reactive power compensation, harmonics
**Słowa kluczowe**: STATCOM, sterowanie ślizgowe, sterowniki PI

## Introduction

Currently, power networks are saturated with asymmetric and non-linear loads and the balance between electrical power production and consumption requires a constant monitoring. In addition, they are growing rapidly and becoming increasingly complex and difficult to control with the integration of decentralized renewable energy sources. Thus, without sophisticated and adequate control devices, many problems can occur on power networks, such as excessive reactive power transit in the power lines and voltage dips between different parts of the network, which results in a decrease of the power quality at the common coupling points (CCPs) and many customers may face severe technical and economic consequences related to poor energy quality [1-4]. Indeed, disturbances such as voltage fluctuations, flickers, harmonics or imbalances can disrupt the operation of many devices and cause the closure of certain industrial processes. Therefore, compensation for these disturbances is necessary and the use of equipment to improve the quality of the electric power has recently increased [5-7].

The traditional electromechanical devices used for power networks control have slow dynamics and are insufficient to answer efficiently the disturbances. The rapid development of power electronics has improved considerably the operating conditions of power networks by providing efficient control devices known by the acronym FACTS (Flexible Alternate Current Transmission Systems) [8, 9]. The latter mainly consist of voltage (or current) converters, linked to capacitors as DC voltage source. Depending on their connection to the power network, these converters can be distinguished as shunt compensators (STATCOM: static compensator), series compensators (SSSC: Static Synchronous Series Compensator) and hybrid compensators (UPFC: Unified Power Flow Controller).

The STATCOM is one widely used for reactive energy compensation and therefore for regulating the voltage at the bus bar to witch it's connected [10]. By use of a DC voltage source, it generates a three-phase AC voltage, synchronous with the power network voltage. Generally, no active power is involved; only the reactive power is exchanged between the STATCOM and the power network, which allows both to correct the power factor and to compensate for voltage drops, thus improving the power quality [11, 12].

The operating principle of the STATCOM is based on an adjustment of the voltage at the common coupling point (CCP) by means of two loops: one internal regulates the current and the other external adjusts the voltage, so as to inject or absorb reactive power with zero active power. It has several advantages such as:

- Efficiency at low voltage: The STATCOM can supply its nominal current even at almost zero voltage [10].
- Good dynamic response: The system responds instantly in real time [10].

Many research works conducted in recent years showed that the efficiency of STATCOM depends largely on the accuracy and robustness of the adopted control technique [2, 13]. Generally, conventional PI controllers are simple and accurate, however, they are strongly affected by parameter variations and they may suffer from stability problems, as shown in [14]. In [15, 16], the authors propose a fuzzy logic control of a D-STATCOM (D-STATCOM: the STATCOM is connected to a low voltage distribution network) and the results are compared to those of a conventional PI control. However, it should be noted that this new technique has a long response time and a noisy steady state. In [17, 18], the authors attempt to improve the performance of a low voltage D-STATCOM (D-STATCOM: the STATCOM is connected to a low voltage distribution grid without use of transformer). For this purpose sliding mode controllers are used in the inner current loops and PI controllers are used in the outer voltage loops.

In the present work, we are interested in improving the performance of a high-voltage electrical network using a STATCOM associated with a step-up transformer. Knowing that the STATCOM control technique is paramount to obtain good dynamic performance, we propose a hybrid method that consists first in a nonlinear sliding mode control for the internal current loops in order to improve the dynamics, then in a classical PI control for external voltage loops. To show the improvement provided by the sliding mode control technique, we compare the obtained results with those of an exclusive PI control.

First, the mathematical model of the STATCOM with the step up transformer is set, then we briefly present the classical PI control, thirdly The SMC technique is well developed, followed by the results analysis, finally the last section concludes the paper.

## Modeling of the STATCOM

The STATCOM can be represented by the equivalent diagram of (Fig.1). For the modeling of the STATCOM, only the busbar of the common coupling point (CCP) is considered and the DC source is assumed to be constant (Fig.1.a). The equivalent circuit of Fig.1.b is therefore an AC voltage source $v_{sh}$ connected to a node of the network by the inductor $L_{sh}$ of the coupling transformer and a resistor $R_{sh}$ representing the ohmic losses of the transformer and the switching losses in the inverter [9]. The current $i_{sh}$ depends on the difference between the node voltage $v_r$ and the adjustable voltage $v_{sh}$ of the STATCOM [15].

The amount of reactive power exchanged between the STATCOM and the network is adjusted by action on the amplitude of the STATCOM voltage $v_{sh}$. This reactive energy is either injected into the network or extracted from the network, which allows regulating the busbar voltage $v_r$ at a wanted value [19].

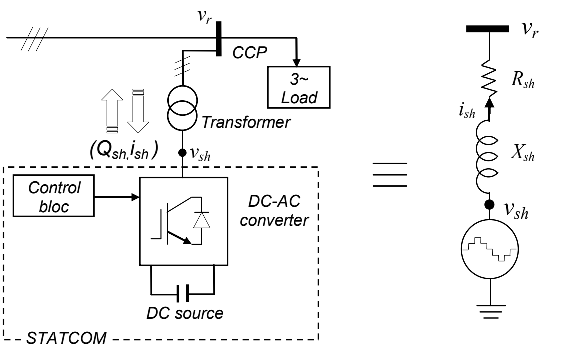


a. Bloc diagram b. Equivalent circuit

Fig.1. Equivalent diagram of a STATCOM

The application of Kirchhoff's laws on the equivalent circuit of Fig.1.b gives:

$$(1)\quad \begin{cases} v_{sha} - v_{ra} = R_{sh} i_{sha} + L_{sh} \dfrac{di_{sha}}{dt} \\ v_{shb} - v_{rb} = R_{sh} i_{shb} + L_{sh} \dfrac{di_{shb}}{dt} \\ v_{shc} - v_{rc} = R_{sh} i_{shc} + L_{sh} \dfrac{di_{shc}}{dt} \end{cases}$$

($v_{ra}, v_{rb}, v_{rc}$): Three phase voltages at the CCP.

($v_{sha}, v_{shb}, v_{shc}$): Three phase voltages at the output of the STATCOM.

($i_{sha}, i_{shb}, i_{shc}$): Three phase shunt current of the STATCOM.

The well known Park transformation allows the transition from a balanced three phase system (*a*, *b*, *c*) to a rotating frame with only two orthogonal axes (*d*, *q*) as follows:

$$(2)\quad \begin{bmatrix} x_d \\ x_q \end{bmatrix} = P(\theta) \begin{bmatrix} x_a \\ x_b \\ x \end{bmatrix}$$

where: ($x_a, x_b, x_c$): Phase components of the three phase system (voltage, current …).

($x_d, x_q$) : Park components. $\theta$: Angle between the phase axis *a* and the rotating axis *d*.

$P(\theta)$: Transformation matrix.

$$[P(\theta)] = \sqrt{\frac{2}{3}} \begin{bmatrix} \cos(\theta) & \cos(\theta - 2\pi/3) & \cos(\theta + 2\pi/3) \\ \sin(\theta) & \sin(\theta - 2\pi/3) & \sin(\theta + 2\pi/3) \end{bmatrix}$$

The inverse Park transformation allows the return to phase components (*a*, *b*, *c*) as follows:

$$(3)\quad \begin{bmatrix} x_a \\ x_b \\ x_c \end{bmatrix} = P(\theta)^{-1} . \begin{bmatrix} x_d \\ x_q \end{bmatrix}$$

$P(\theta)^{-1}$: Inverse transformation matrix.

$$[P(\theta)] = \sqrt{\frac{2}{3}} \begin{bmatrix} \cos(\theta) & \sin(\theta) \\ \cos(\theta - 2\pi/3) & \sin(\theta - 2\pi/3) \\ \cos(\theta + 2\pi/3) & \sin(\theta + 2\pi/3) \end{bmatrix}$$

Considering $\theta = 2\pi f t$ ($f$: frequency of the grid currents), the application of park transformation to equation (1) gives [20]:

$$(4)\quad \begin{cases} v_{shd} - v_{rd} = R_{sh} i_{shd} + L_{sh} \dfrac{di_{shd}}{dt} - \omega L_{sh} i_{shq} \\ v_{shq} - v_{rq} = R_{sh} i_{shq} + L_{sh} \dfrac{di_{shq}}{dt} + \omega L_{sh} i_{shd} \end{cases}$$

Then, we can write the following state equation of the STATCOM:

$$(5)\quad \frac{d}{dt} \begin{bmatrix} i_{shd} \\ i_{shq} \end{bmatrix} = \begin{bmatrix} -\dfrac{R_{sh}}{L_{sh}} & \omega \\ -\omega & -\dfrac{R_{sh}}{L_{sh}} \end{bmatrix} \begin{bmatrix} i_{shd} \\ i_{shq} \end{bmatrix} - \frac{1}{L_{sh}} \begin{bmatrix} v_{shd} - v_{rd} \\ v_{shq} - v_{rq} \end{bmatrix}$$

$\begin{bmatrix} v_{shd} \\ v_{shq} \end{bmatrix} = \begin{bmatrix} u_1 \\ u_2 \end{bmatrix}$ : Input vector of the system.

$\begin{bmatrix} i_{shd} \\ i_{shq} \end{bmatrix}$ : State variables of the system.

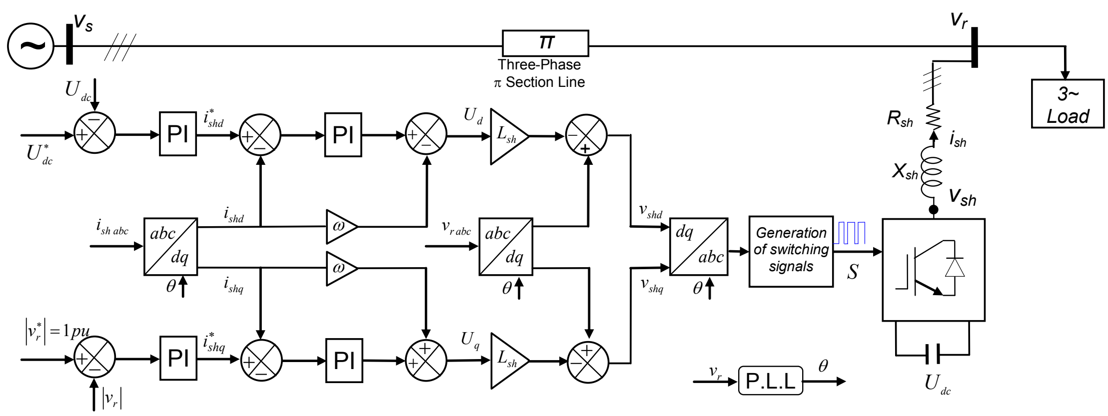


Fig.2. Bloc diagram of PI control strategy

**Classical PI control strategy**

This strategy is well known in the literature; it is based on two internal and two external loops, as shown in Fig.2. The external loops allow each to adjust the active and reactive currents $i^*_{shd}$ and $i^*_{shq}$, while the two inner loops each achieve a PI control of reference voltages $v^*_{shd}$ and. $v^*_{shq}$ In the first external loop, the measured DC voltage $U_{dc}$ is compared to its reference and an active reference current $i^*_{shd}$ is generated [8] and in the second loop, the reactive current is generated by comparing the coupling voltage $v_r$ with its reference $v^*_r$. The outputs of the two internal controllers give the reference voltages $v^*_{shd}$ and $v^*_{shq}$ using a PLL (phase-locked loop). Finally, the phase voltages are calculated using the inverse Park transform, and used for the generation of switching signals (Fig.2).

The synthesis of the PI controllers is based on the block diagram presented in Fig.3 and the pole compensation method is used to determine the PI parameters. To obtain a satisfactory adjustment in the inner loops, a decoupling between the active and reactive currents is required.

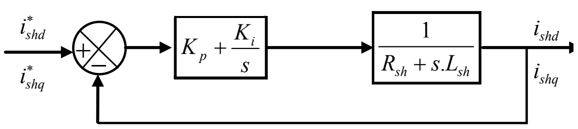


Fig.3. Block diagram of PI control of $i_{shd}$ and $i_{shq}$ currents

**Proposed Sliding mode control of the STATCOM**
**Sliding mode control technique**

Sliding mode control (SMC) has been very successful in recent years due to the simplicity of its implementation and its robustness to system uncertainties and external process disturbances [17, 20]. This technique forces the state trajectory of the considered system to reach and then slide on a desired surface using appropriate switching logic [20]. The implementation of this technique requires three steps:

**First step:** Choice of the sliding surface.
Let' consider a nonlinear system described by the following state equation (6):

(6) $$\begin{cases} \dot{x} = f(x) + g(x).u \\ x \in \Re^n \ , u \in \Re^m \end{cases}$$

Where, $f(x)$ and $g(x)$ are two nonlinear functions.

Note that the number of sliding surfaces is equal to the number of inputs. Thus, such input vector $u$ of dimension $m$ requires $m$ sliding surfaces.

As proposed by [21], the general shape of the sliding surface that ensures the convergence of a state variable $x$ to its set value $x^*$, is described by the following expression:

(7) $$S(x) = \left(\frac{\partial}{\partial t} + \lambda\right)^{r-1} e(x)$$

Where:
$e(x)$: The difference between the variable to be regulated and its reference.
$\lambda$ : Positive constant.
$r$ : Relative degree, equal to the number of derivatives of the output to make the command appear.

**Second step:** Verification of de convergence condition.
The condition of convergence is defined by the Lyapunov equation, which makes the surface attractive and invariant:

(8) $$S(x)\dot{S}(x) \le 0$$

**Third step:** Determination of the control law.
The control law which allows bringing the output to the sliding surface is determined by use of the equivalent command $u_{eq}$ and the attractive command $u_c$ as follows:

(9) $$u = u_c + u_{eq}$$

$u_c$ : as attractive command, used to bring the controlled variable to the sliding surface.
$u_{eq}$ : equivalent command, used to maintain the controlled variable on the sliding surface.
The derivative of the sliding surface is expressed as follows:

(10) $$\frac{dS}{dt} = \frac{dS}{dx}.\frac{dx}{dt}$$

Replacing $\frac{dx}{dt}$ by its expression in Eq.(6), equation (10) becomes:

(11) $$\frac{dS}{dt} = \frac{dS}{dx}\left\{f(x) + g(x).u_{eq}\right\} + \frac{dS}{dx} g(x).u_c = 0$$

This control law is applied in the two following situations:

- Once the system has reached the sliding surface, the attractive command is canceled ($u_c$ = 0) and the equivalent command can be expressed as follows:

(12) $$u_{eq} = -\left\{\frac{dS}{dx} g(x)\right\}^{-1} \left\{\frac{dS}{dx} f(x)\right\}$$

- As long as the system has not yet reached the sliding surface, the attractive command $u_c$ is set as follows:

(13) $$u_c = -k_1 S - k_2 \operatorname{sign}(S(x))$$

Where $k_1$ and $k_2$ are positive constants.

To eliminate the Chattering problem, we approximate the nonlinear sign function " $sign(.)$ " in equation (13), by the smooth function " $\tanh(.)$ " as in [17, 20], which allows avoiding the abrupt change from -1 to +1 imposed by the sign function, thus:

(14) $$\operatorname{sign}(S(x)) \approx \tanh(S(x))$$

**Application to the STATCOM**

In this section, the SM controller is applied to the STATCOM as an alternative to the two internal PI loops of the reference voltages $v_{shd}$ and $v^*_{shq}$ , (Fig.4).

Since two variables need control, two sliding surfaces are required as follows:

(15) $$S_1 = \left(\frac{d}{dt} + \lambda_1\right)\int_0^t e_1$$

(16) $$S_2 = \left(\frac{d}{dt} + \lambda_2\right)\int_0^t e_2$$

Where:

(17) $$e_1 = i^*_{shd} - i_{shd}$$

(18) $$e_2 = i^*_{shq} - i_{shq}$$

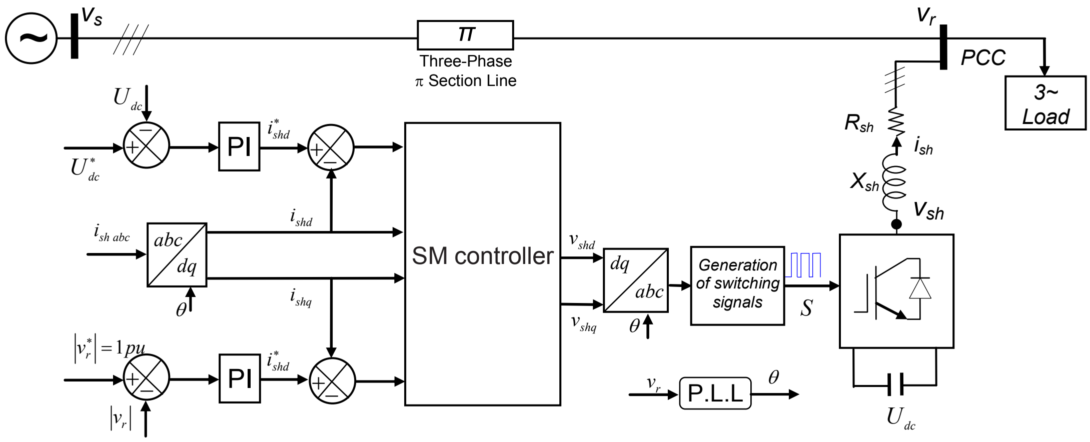


Fig.4. Bloc diagram of SM control strategy

By considering the commands $u_1 = v_{shd}$ and $u_2 = v_{shq}$, state equation (5) becomes:

(19) $$\frac{d}{dt} i_{shd} = -\frac{R_{sh}}{L_{sh}} i_{shd} + \omega . i_{shq} - \frac{1}{L_{sh}} v_{rd} + \frac{1}{L_{sh}} u_1$$

(20) $$\frac{d}{dt} i_{shq} = -\frac{R_{sh}}{L_{sh}} i_{shq} - \omega . i_{shd} - \frac{1}{L_{sh}} v_{rq} + \frac{1}{L_{sh}} u_2$$

Where:

(21) $$u_1 = u_{eq1} + u_{c1}$$

(22) $$u_2 = u_{eq2} + u_{c2}$$

By introducing equations (17) and (18) into equations (15) and (16) respectively, the derivatives of the sliding surfaces are obtained as follows:

(23) $$\dot{S}_1 = \dot{i}_{shq}^* - \dot{i}_{shq} + \lambda_1 . e_1 - \lambda_1 . e_1(0)$$

(24) $$\dot{S}_2 = \dot{i}_{shq}^* - \dot{i}_{shq} + \lambda_2 . e_2 - \lambda_2 . e_2(0)$$

Then, introducing equation (19) in (23) and equation (20) in (24), we obtain:

(25) $$\dot{S}_1 = \dot{i}_{shd}^* + \frac{R_{sh}}{L_{sh}} i_{shd} - \omega . i_{shq} + \frac{1}{L_{sh}} v_{rd} - \frac{1}{L_{sh}} u_1 + \lambda_1 . e_1 - \lambda_1 . e_1(0)$$

(26) $$\dot{S}_2 = \dot{i}_{shq}^* + \frac{R_{sh}}{L_{sh}} i_{shq} + \omega . i_{shd} + \frac{1}{L_{sh}} v_{rq} - \frac{1}{L_{sh}} u_2 + \lambda_2 . e_2 - \lambda_2 . e_2(0)$$

Taking into account the two conditions $\dot{S}_1 = \dot{S}_2 = 0$ and $u_{c1} = u_{c2} = 0$, the equivalent commands $u_{eq1}$ and $u_{eq2}$ can be obtained as follows:

(27) $$u_{eq1} = L_{sh} \dot{i}_{shd}^* + R_{sh} i_{shd} - L_{sh} \omega i_{shq} + v_{rd} + L_{sh} \lambda_1 (e_1 - e_1(0))$$

(28) $$u_{eq2} = L_{sh} \dot{i}_{shq}^* + R_{sh} i_{shq} + L_{sh} \omega i_{shd} + v_{rq} + L_{sh} \lambda_2 (e_2 - e_2(0))$$

The attractive commands $u_{c1}$ and $u_{c2}$ are calculated so as to satisfy the following conditions:

(29) $$\begin{cases} \dot{S}_1 = -\alpha_1 S_1 - \beta_1 \, sign(S_1) \\ \dot{S}_2 = -\alpha_2 S_2 - \beta_2 sign(S_2) \end{cases}$$

Using the expressions of $u_{eq1}$ and $u_{eq2}$ (Eq.(27) and Eq.(28)) in Eq.(21) and Eq.(22) and then replacing the obtained expressions of $u_1$ and $u_2$ in Eq.(25) and Eq.(26) we obtain:

(30) $$\dot{S}_1 = -\frac{1}{L_{sh}} u_{c1}$$

(31) $$\dot{S}_2 = -\frac{1}{L_{sh}} u_{c2}$$

Replacing $\dot{S}_1$ and $\dot{S}_2$ by their expressions (Eq.(30) and Eq.(31)) in Eq.(29), it becomes:

(32) $$u_{c1} = -\alpha_1 L_{sh} S_1 - \beta_1 L_{sh} \, sign\ (S_1)$$

(33) $$u_{c2} = -\alpha_2 L_{sh} S_2 - \beta_2 L_{sh} \, sign(S_2)$$

Finally, equations (32) and (33) are introduced in equations (21) and (22), we obtain:

(34) $$u_1 = L_{sh} \dot{i}_{shd}^* + R_{sh} i_{shd} - L_{sh} \omega . i_{shq} + v_{rd} + L_{sh} \lambda_1 . (e_1 - e_1(0)) - \alpha_1 L_{sh} S_1 - \beta_1 L_{sh} \, sign(S_1)$$

(35) $$u_2 = L_{sh} \dot{i}_{shq}^* + R_{sh} i_{shq} + L_{sh} \omega . i_{shd} + v_{rq} + L_{sh} \lambda_2 . (e_2 - e_2(0)) - \alpha_2 L_{sh} S_2 - \beta_2 L_{sh} \, sign(S_2)$$

## Simulations and results analysis

### Simulations

The single-line diagram of the power network used to validate the operation of the proposed STATCOM is shown in Fig.5.

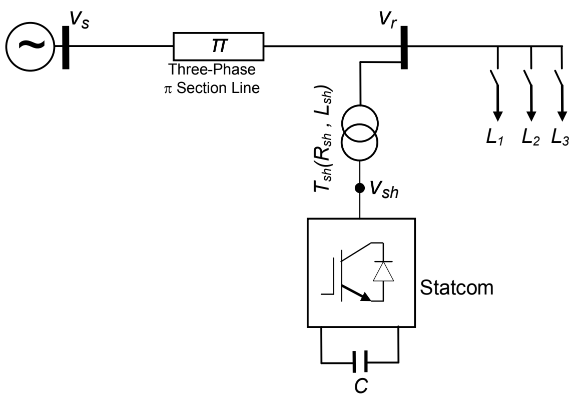


Fig.5.Single-line diagram of the studied network

The considered network consists of a 400 KV generator with a nominal power of 1000 MVA and a power line of 100 km modeled in $\pi$. Transformer $T_{sh}$ lowers the voltage from 400 kV (mains voltage) to 20 kV (output voltage of the STATCOM). Simulations are performed in per unit system by using $S_B$ = 1000 MVA and $U_B$ = 400 kV as base values, while the voltage of the generator busbar is $V_S$ = 1.0 pu.

Three loads (L1, L2 and L3) are connected to the busbar "$r$" as follows:

- Initially ($t$ < 0), no load is connected, all breakers are open.
- At time ($t$ = 0 s), an inductive load (L1: $P_1$ = 1.0 pu and $Q_1$ = 0.4 pu) is connected.
- At time ($t$ = 0.5 s), a second inductive load L2 is added (L2: $P_2$ = 0.5 pu, $Q_2$ = 0.4 pu).
- At time ($t$ = 1 s), a third capacitive load L3 is also added (L3: $P_3$ = 0.3 pu, $Q_{3c}$ = 0.2 pu, $Q_{3l}$ = 0.01 pu).
- Finally at time ($t$ = 1.5 s) the inductive loads L1 and L2 are disconnected; only the capacitive load L3 is maintained.

**Results analysis**

Fig.6 shows the voltage drop caused by the inductive load L2 at time $t$ = 0.5 s at both source and load bus bars. This voltage drop is naturally damped by the capacitive load connection L3 at time $t$ = 1 s. Finally, the disconnection of all inductive loads in the last transition at time $t$ = 1.5 s, resulted in a capacitive load flow, which caused a surge at the two busbars. Note that the effect of the load variation on the source busbar is attenuated.

Fig.7 shows the resulting phase shift between the voltage and the current in both cases: inductive load between $t$ = 0.9 s and $t$ = 0.96 s (Fig.7.a) and capacitive load between $t$ = 1.9 s and $t$ = 1.96 s (Fig.7.b).

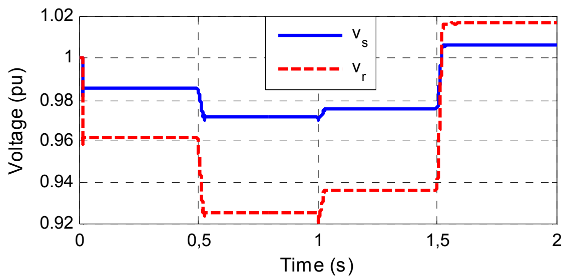


Fig.6. Source voltage $v_s$ and load voltage $v_r$ before compensation

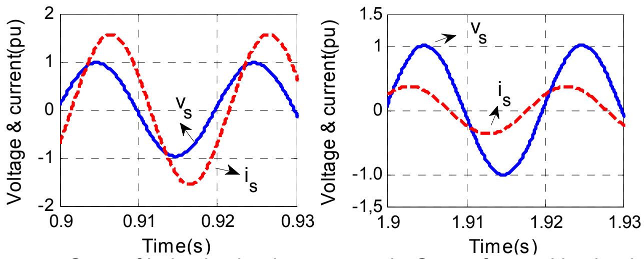


a. Case of inductive load b. Case of capacitive load

Fig.7.Grid voltage $v_s$ and current $i_s$ before compensation

Figs.8-13 show some simulation results after compensation. The proposed SMC control is compared to conventional PI control.

Fig.8.a (PI control) and Fig.8.b (SM control) show that the STATCOM provides reactive current ($i_{shq} > 0$) for inductive loads and absorbs reactive current ($i_{shq} < 0$) for capacitive loads. Indeed, from $t$ = 0 s to $t$ = 0.5 s, only the inductive load L1 is connected; the STATCOM injects a small amount of reactive power Qsh ≈ 0.45 pu in order to maintain the load voltage $v_r$ at 1.0 pu. With the addition of the inductive load L2 at $t$ = 0.5 s, more reactive power is then required and the STATCOM injects Qsh ≈ 0.92 pu as shown in Fig.9.b. By connecting the capacitive load L3 at $t$ = 1 $s$, the reactive power provided by the STATCOM decreases from Qsh ≈ 0.92 pu to Qsh = 0.8 pu because of the capacitive effect of this load (Fig.9.b). In the last step ( $t$ > 1.5 s), only the capacitive load is connected, an overvoltage appears on the load busbar and forces the STATCOM to operate in inductive mode to absorb the reactive power from the network, in order to maintain $v_r$ at its nominal value, (Fig.9.b); during this step, $i_{shq}$ changes sign and becomes negative. We notice the low value of active power consumed by the STATCOM to compensate for losses in the power switches of static converter (Fig.9.a).

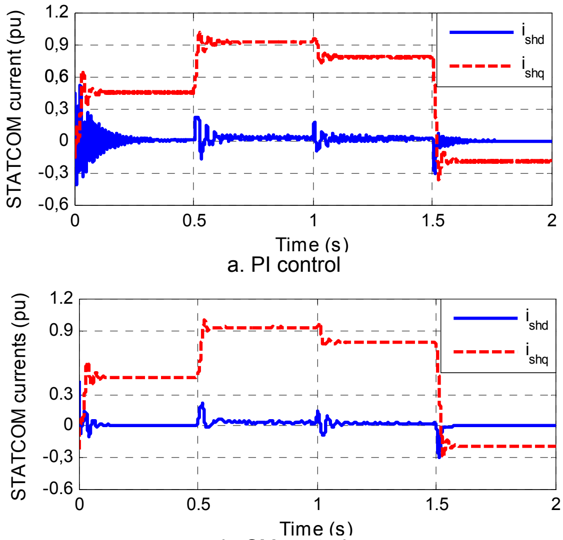


b. SM control

Fig.8. STATCOM currents $i_{shd}$ and $i_{shq}$ after compensation

Fig.10.b shows that the voltage of the load busbar is well regulated at its nominal value $v_r$ = 1.0 pu. In addition, a positive effect is noted on the voltage $v_s$, which becomes very close to its nominal value, (Fig.10.a).

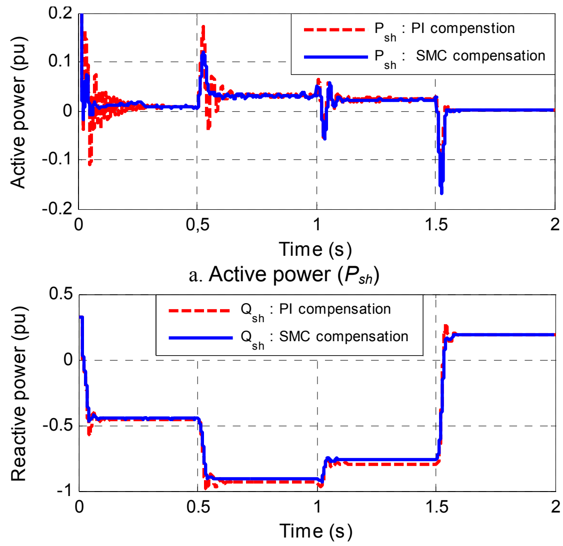


b. Reactive power ($Q_{sh}$)

Fig.9. Active and reactive power after PI and SMC compensation

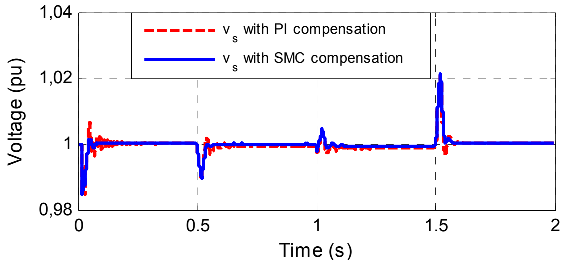


a. Source voltage ( $v_s$ )

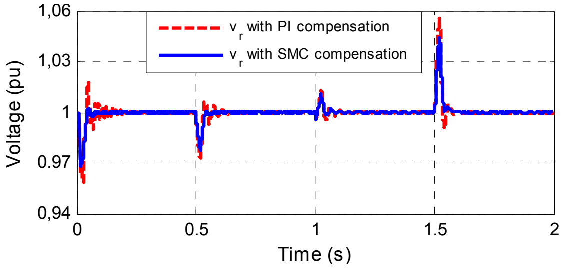


b. Load voltage ( $v_r$ )

Fig.10. Source voltage $v_s$ and load voltage $v_r$ after PI and SMC compensation

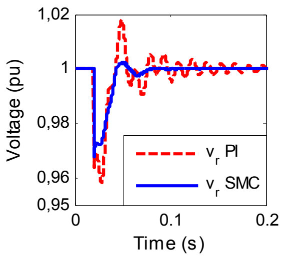


a.Transient at $t$ = 0 s

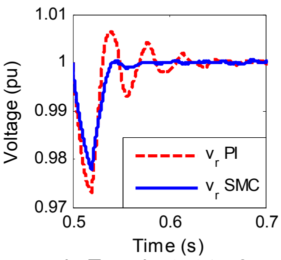


b. Transient at $t$ = 0.5 s

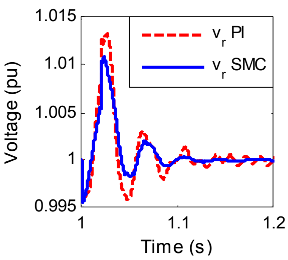


c.Transient at $t$ = 1 s

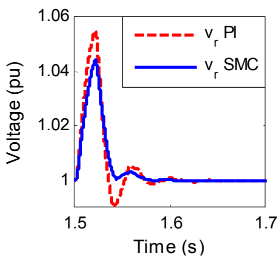


d. Transient at $t$ = 1.5 s

Fig.11. Transients of load voltage $v_r$ for both PI and SMC compensations

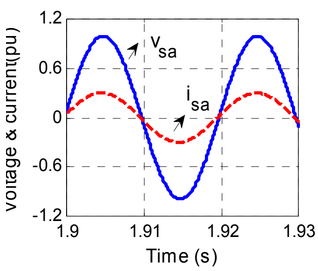


a. PI compensation

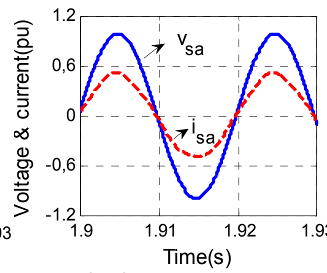


b. SMC compensation

Fig.12. Grid voltage vs and current $i_s$ after compensation

In addition, Figs.8-10 show that the proposed SM control is much more effective than PI control. To better appreciate this effectiveness, Figs.11.a-11.d show the dynamic behavior of $v_r$ voltage under the two control techniques; it appears clearly that SM control gives faster dynamics with less oscillation than PI control.

As an indication, Figs.12.a-12.b show that the voltage $v_s$ and the current $i_s$ are in phase in steady state after compensation; this indicates that there is no transit of reactive power between the source and the load after compensation.

Globally, Figs.8-11 show that the proposed SM control is much more effective than PI control. Indeed, SM control gives faster dynamics with less oscillation than PI control.

Moreover, a comparison of the harmonic spectra of the source current $i_S$ for the two control techniques (PI and SM) shows a lower THD (Total Harmonic Distortion) for the SM control, (Fig.13).

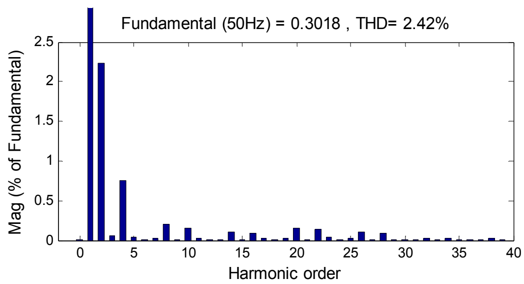


a. PI compensation

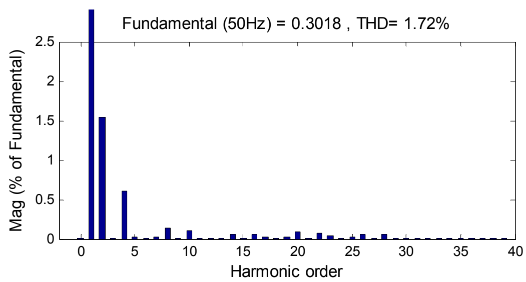


b. SMC compensation

Fig.13. Harmonic spectrum of the source current $i_s$

To carry out an accurate comparison between the SM control and the PI control, we define the following two cost functions: [22]:

(36) $$J_1 = 0.5\sum_{i=1}^{p}\left(u_1^2 + u_2^2\right)$$

(37) $$J_2 = 0.5\sum_{i=1}^{p}\left(e_1^2 + e_2^2\right)$$

Where:

- $p$ is the length of each of the control vector $u$ and the error vector $e$ during a given simulation time.
- Function $J_1$ defines an energy performance criterion.
- Function $J_2$ defines a criterion of control efficiency.

Note:

Table 1 compares between the two control techniques; it appears clearly that SM control is more efficient than PI control according to the above two criteria.

Table 1. Comparison between the two control techniques $p$ = 61441

| Controller | $J_1$ | $J_2$ |
|---|---|---|
| SM Controller | 103.22 | 2.02 $10^4$ |
| PI controller | 197.06 | 6.00 $10^4$ |

## Conclusion

The main purpose of this paper is the improvement of the performance of a STATCOM by use of a hybrid control technique based on SM control and PI control. This new control technique is developed and adapted to the proposed system. Finally the simulation results show a substantial improvement in system performance both in terms of STATCOM dynamics and network power quality.

***Acknowledgements***: *Our thanks go to the DGRSDT (Directorate-General for Scientific Research and Technological Development) at the Ministry of Higher Education and Scientific Research of Algeria for its support.*

***Authors***: *Hassen Belila. University of Oum El Bouaghi, Algeria, Science and Applied Sciences Faculty, 04000 Oum El Bouaghi, Algeria, E-mail: hassenbelila@yahoo.fr; Nasserdine Boudjerda. University of Jijel, Algeria, Faculty of science and Technology, B.P 98 Ouled Aissa Jijel, Algeria, E-mail: n_boudjerda@yahoo.fr; Ahsene Boubakir. University of Jijel, Algeria, Faculty of science and Technology, B.P 98 Ouled Aissa Jijel, Algeria; E-mail: ah_boubakir@yahoo.fr; Imen Bahri.* University of Paris-Saclay, Group of Electrical Engineering, Paris (GeePs), UMR CNRS 8507, 3 rue Joliot-Curie, Plateau de Moulon 91192 Gif-sur-Yvette CEDEX, France, *E-mail: imen.bahri@centralesupelec.fr*.

## REFERENCES

[1] Wo B., Lang Y., Zargari N., Kouro S., Power conversion and control of wind energy system, John Wiley and sons Publication, *IEEE Press*, July 2011.
[2] Tremblay E., Atayde S., Chandra A., Comparative Study of Control Strategies for the Doubly Fed Induction Generator in Wind Energy Conversion Systems: A DSP-Based Implementation Approach, *IEEE Trans*. on Sust. Energy, Vol. 2 (2011), No. 3.
[3] Moghbel M., Masoum M.A.S., Optimal Sizing, Siting and Operation of Custom Power Devices With STATCOM and APLC Functions for Real-Time Reactive Power and Network Voltage Quality Control of Smart Grid, IEEE Trans. Smart Grid, 9 (2018), No. 6.
[4] Moghe R., Divan D., Turning Distribution Feeders Into STATCOMs, *IEEE Trans*, Ind, Appl., 53 (2017), No. 2.
[5] Zhang Y., Wu X. J., High Order Voltage and Current Harmonic Mitigation Using the Modular Multilevel Converter STATCOM, *IEEE Trans*, Ind, Electr, 5 (2017), No. 19.
[6] Padiyar K., FACTS controllers in power transmission and distribution, New Age International, 2007.
[7] Feola L., Langella R., Papic I., Testa A., Selective Interharmonic Compensation to Improve Statcom Performance for Light Flicker Mitigation*, IEEE Trans On* Power Delivery, vol. 33, No. 5, OCTOBER 2018.
[8] Sen K.K., Sen M.L., Introduction to FACTS controllers: theory, modeling, and applications, John Wiley & Sons, 54 (2009).
[9] Xu, L., Han Y., Passivity-based Controller Design and Stable Control Region Analysis of the Cascaded DSTATCOM, *Przeglad Elektrotechniczy*, 88 (2012), nr 3b, 140-148.
[10] FALEHI A.D., Mitigation of Power System Oscillations Using STATCOM-Based PDD Damping controller, *Przeglad Elektrotechniczy*, 88 (2012), nr 12a, 275-279.
[11] Hingorani N.G., Gyugyi L., Comparative Analysis of 6, 12 and 48 Pulse T-STATCOM*, IEEE 7th PIICON* Nov. 2016.
[12] Mosaad M.I., Model reference adaptive control of STATCOM for grid integration of wind energy systems, *IET Electr*, Power Appl., Vol. 12 (2018), Iss. 5, pp. 605-613
[13] Abad G., Lopez J., Rodriguez M.A., Marroyo L., Lwanski G., Doubly fed induction machine modelling and control for wind energy generation, *IEEE press.,* John Wiley, 2011.
[14] Yao X., Fangxing L., Adaptive PI Control of STATCOM for Voltage Regulation, *IEEE Trans.* P. Delivery., Vol. 29 (2014), No. 3.
[15] Routray S.K., Nayak N., Rout P.K., A Robust Fuzzy Sliding Mode Control Design for Current Source Inverter based STATCOM Application, *Procedia* Technology 4 (2012 ), pp. 342 – 349.
[16] Ajami A., Taheri N., A Hybrid Fuzzy/LQR Based Oscillation Damping Controller Using 3-level STATCOM, Int. J. Comp. and Elect. Eng., vol. 3 (2011), no. 2, pp.184-189.
[17] Yunhao H., Yuanyun S., Han Z.,Yang M., Sliding mode reactive power control of isolated wind-disel hybrid power system based on STATCOM, 37th Chinese Control Conference Jul. 2018, Wuhan, China.
[18] Ziaeinejad S., Mehrizi-Sani A., Design Tradeoffs in Selection of the DC-Side Voltage for a D-STATCOM, *IEEE Trans* on Power Delivery, Vol. 33 (2018), No. 6.
[19] Hamoud F., Doumbia M.L., Cheriti A., Hybrid PI-Sliding mode control of a voltage source converter based STATCOM, 16th International *PEMC* 2014, Sept. 2014 Antalya, Turkey.
[20] Touil S. A., Boudjerda N., Boubakir A., El Khamlichi D. K., A sliding mode control and artificial neural network based MPPT for a direct grid-connected photovoltaic source, Asian Journal of Control, vol. 21 (2019), special issue, pp. 1–14.
[21] Ruiz-Zea C.A., Jimenez-Rodriguez E., Canedo-Castaneda, J.M., Loukianov A.G., Sanchez-Torres J.D., Second Order Sliding Mode Control of a STATCOM with Saturated Inputs, 15th International Conference on Electrical Engineering, Computing Science and Automatic Control (CCE), Mexico City, Mexico. Sept., 2018.
[22] Boubakir A., Boudjema F., Boubakir C., Labiod S., A Fuzzy Sliding Mode Controller Using Nonlinear Sliding Surface Applied to the Coupled Tanks System, International Journal of Fuzzy Systems, Vol. 10 (2008), No. 2.